Searches for physics beyond the Standard Model at the Tevatron

ALBERTO ANNOVI, for the CDF and D0 Collaborations

INFN Laboratori Nazionali di Frascati, via E. Fermi 40, 00044 Frascati (RM), Italy
E-mail: annovi@fnal.gov

Abstract. During the last 10 years, the Fermilab Tevatron has produced $p\bar{p}$ collision at a centre-of-mass energy of 1.96 TeV that the CDF and D0 Collaborations have scrutinized looking for new physics in a wide range of final states. Here, recent updates of new physics searches are reported using a data sample of up to 9 fb^{-1}.

Keywords. Fermilab; CDF; D0; searches.

PACS Nos   11.30.Pb; 12.15.–y; 12.38.Qk; 14.80.–j

1. Introduction

Because of the limitations of the Standard Model (SM), several extensions such as supersymmetry (SUSY), grand unified theories, and string theory have been promoted. Extensions to the Standard Model augment the existing particle content, leading to enhanced production of many final states at the colliders.

During the last 10 years, the Fermilab Tevatron has produced $\approx 8 \times 10^{13}$ $p\bar{p}$ collision at a centre-of-mass energy of 1.96 TeV at each of the two interaction points. The CDF [1,2] and D0 [3,4] Collaborations have scrutinized these collisions searching for signals of physics beyond the Standard Model. The new physics search program at the Tevatron spans from supersymmetry and extra dimensions to more exotic and model-independent searches. Here we report recent updates of new physics searches. In order to simplify the notation, the convention $c = 1$ is used throughout this paper.

1.1 *Background modelling*

A crucial element of all data analyses that search for new physics is a detailed modelling of all the backgrounds. We can summarize the strategy used to model the background as follows. For the electroweak processes (diboson, top, W/Z+jets), the distributions of the kinematical variables of interest are obtained from Monte Carlo-based calculations. The cross-sections of these processes are normalized to the most recent theoretical calculations at next-to-leading order (NLO) or next-to-next-to-leading order (NNLO). The background from QCD multijet processes are usually extracted from the data itself using

background-enriched data samples. In this way, the multijet background is determined with a data-driven approach reducing the complexity and the systematic uncertainties that would be associated with a Monte Carlo generation of QCD multijet processes. For the same reasons, the normalization of the multijet background is extracted from the data. For analyses where the W+jets is the dominant background, the event yield for W+jets cannot be predicted with an accuracy comparable with the statistical error. In order to improve the sensitivity to new phenomena, the normalization of W+jets is usually fitted to data.

The Monte Carlo generators that are mostly used are:

- $WW/WZ/ZZ$: PYTHIA [5] is used by CDF and D0
- $t\bar{t}$: PYTHIA is used by CDF and ALPGEN [6] is used by D0
- single-top: PYTHIA is used by CDF and COMPHEP [7] is used by D0
- W+jets and Z+jets: ALPGEN is used by CDF and D0

The parton distribution functions used are: CTEQ5L [8] for CDF and CTEQ6L1 [9] for D0. The event generators are combined with showering from PYTHIA to obtain observable particles. The generated events are then fed to a detector simulation that is based on GEANT3. We use modelling of the known processes to test the Standard Model [10] in a multitude of final states where a new phenomenon could be hiding.

2. Leptoquarks

Many extensions of the SM predict the existence of particles that directly connect the lepton and quark sectors. By combining leptons and quarks in multiplets of a larger symmetry group, they are expected to interact through new mediating bosons called leptoquarks (LQ) [11]. The D0 Collaboration searches for pair production of massive scalar leptoquarks in a data sample of 5.4 fb^{-1} [12]. Leptoquarks are assumed to couple only to the first generation, with branching ratios: BR(LQ $\rightarrow eq$) $= \beta$ and BR(LQ $\rightarrow \nu q$) $= 1 - \beta$. The final state used for this search has one LQ decaying into eq and the other into νq. Events with one electron, two jets and missing transverse energy are selected. The main background is W/Z+jets production that is suppressed requiring the transverse mass of the electron and neutrino to be greater than 110 GeV. The other backgrounds are diboson production, top production and multijet events. To further suppress the backgrounds, the sum of the reconstructed LQ masses is required to be greater than 350 GeV. In the remaining data sample, massive leptoquarks would appear as an excess of events with large transverse S_T, the scalar sum of the transverse energy of all objects including $\not{E}_T$. The S_T distribution, shown in figure 1a, is used as the discriminating variable. The data are found to be in good agreement with the SM background. The signal corresponding to leptoquarks with a mass of 260 GeV is also shown. Limits on the BR(LQ $\rightarrow eq$) $= \beta$ as function of the LQ mass are shown in figure 1b. LQ masses below 326 GeV are excluded for $\beta = 0.5$.

3. RS gravitons

The D0 Collaboration searches for Randall–Sundrum (RS) [13] gravitons (G) in the diphoton and dielectron final states using a data sample of 5.4 fb^{-1}. A signal would
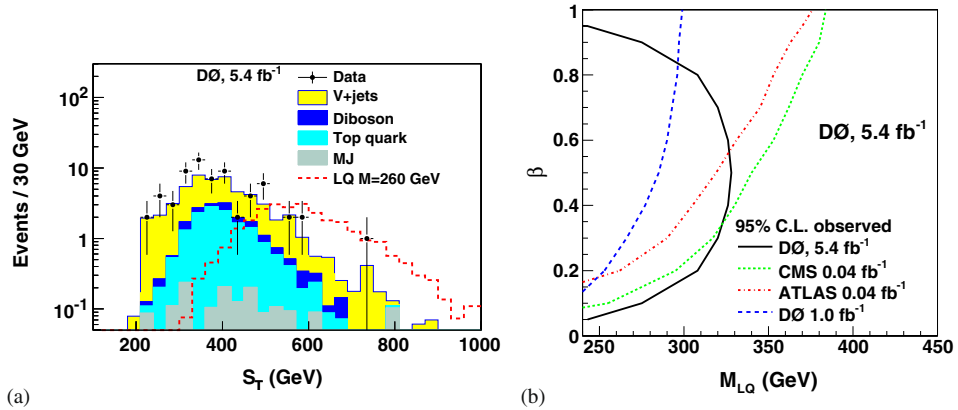
Figure 1. (**a**) Distribution of S_T, the scalar sum of transverse energy of all objects including $\not{E}_T$. (**b**) Limits on the BR(LQ $\rightarrow$ eq) = β as function of the LQ mass.

appear as a resonance in the diphoton or dielectron invariant mass. No excess is observed over the SM prediction and RS gravitons with graviton mass less than 1050 GeV are excluded for $k/M_{\text{Planck}} = 0.1$ [14], where k is the curvature scale of the extra dimension and M_{Planck} is the Planck mass.

The CDF Collaboration searches for RS gravitons in the diphoton and dielectron final states [15] and recently added a new search in the dimuon final state [16] using a data sample of 5.7 fb^{-1}. Again, the data are in good agreement with the SM expectation in all channels. Combining the three channels, RS gravitons with $M_G < 1111$ GeV are excluded for $k/M_{\text{Planck}} = 0.1$ [16].

4. Search for a WW/WZ resonance

The D0 Collaboration searches for resonant WW and WZ production [17]. A sequential Standard Model (SSM) [18] W' boson is used as benchmark for a WZ resonance and a RS graviton resonance for the WW final state. The experimental final state for this search are either two leptons or one lepton plus $\not{E}_T$, and at least one jet. The vector boson decaying into jets can be reconstructed either as two jets or as a 'fat jet' with large mass. Figure 2 shows the reconstructed WZ mass for the two-lepton channel (figure 2a) and the WW or WZ mass for the lepton+$\not{E}_T$ channel (figure 2b). The data are found to be in good agreement with the SM background. Figure 3 shows the cross-section times branching ratio limits for a W' resonance and for the RS graviton.

5. Search for ZZ resonance

5.1 *CDF search for ZZ resonance*

The CDF Collaboration searches for resonances decaying to a ZZ pair [19]. New physics could affect ZZ production in different ways. In models containing large extra
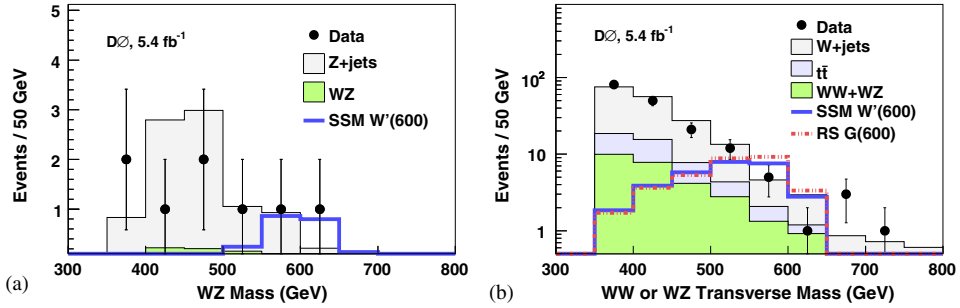
Figure 2. Reconstructed WZ mass for the two-lepton channel (**a**) and the WW/WZ mass for the lepton+E_T channel (**b**).
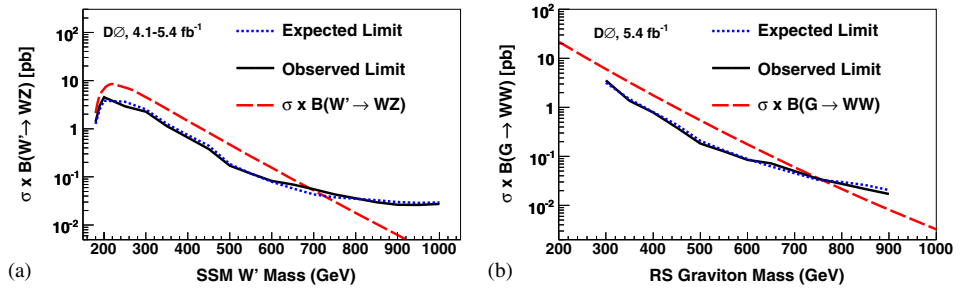

Figure 3. Limits on W' decaying to WZ (**a**) and limits on Randall–Sundrum graviton (**b**).

dimensions, the ZZ production cross-section is increased through loop corrections [20]. Resonances appearing at high mass such as a Higgs boson or Randall–Sundrum (RS) graviton [13] could decay manifestly to two Z bosons.

Three final states are analysed, corresponding to the different Z boson decay modes $ZZ \rightarrow l^+l^-l^+l^-$, $ZZ \rightarrow l^+l^-\nu\bar{\nu}$, and $ZZ \rightarrow l^+l^-jj$, where l is an electron or muon and j is a hadronic jet. These three channels have different signal-to-background ratios and allow an overconstrained search. The $l^+l^-l^+l^-$ final state has the smallest background; however, depending on the resonance mass, the best single-channel sensitivity is provided by either the $ZZ \rightarrow l^+l^-jj$ or $ZZ \rightarrow l^+l^-\nu\bar{\nu}$ channels.

For the $l^+l^-l^+l^-$ final state, events with four leptons with $p_T > 15$ GeV including one trigger lepton with $p_T > 20$ GeV are selected. Pairs of opposite sign leptons are retained if they satisfy $76 < m_{ll} < 106$ GeV. In the data sample of 6 fb^{-1}, eight candidates are found, to be compared with an expected ZZ background of 5.8 events. The non-ZZ background is negligible and estimated to be less than 0.01 events. The mass (m_{ZZ}) distribution of the candidates is shown in figure 4a. Four of the eight candidates cluster within 20 GeV of mass and are all compatible with a mass of 327 GeV. The probability that this unexpected feature is due to a fluctuation of the background is evaluated *a posteriori*. The probability of observing four or more ZZ events that have $m_{ZZ} > 300$ GeV, with m_{ZZ} values of at least four of them within a 20 GeV window (which corresponds to approximately $\pm 2\sigma$ in resolution) is in the range $(2.3-5.2) \times 10^{-4}$, where the range comes from different

(a)

(b)
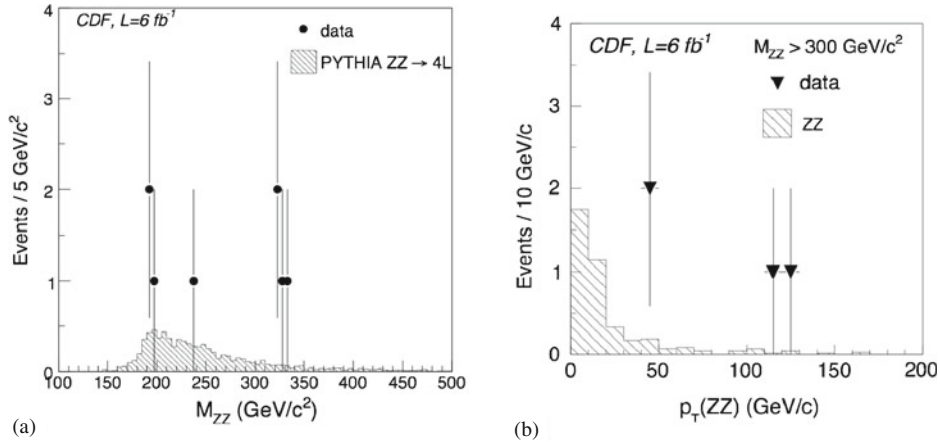
Figure 4. (**a**) m_{ZZ} distribution for the eight ZZ candidates. The background is normalized to the expected 5.8 events. (**b**) Transverse momentum distribution for candidates with $m_{ZZ} > 300$ GeV.

event generators. These events are investigated in detail in order to verify whether they are compatible with real ZZ decays. No suspicious features are found. Figure 5 shows the invariant mass distribution of each reconstructed Z boson. Figure 4b shows the p_T distribution of the ZZ pairs. For the four candidates with $m_{ZZ} > 300$ GeV, the data tend to be harder than the expected background.

Candidate events for the $ZZ \rightarrow l^+l^-\nu\nu$ process must have two leptons and $\not{E}_T > 100$ GeV. The events with $\not{E}_T < 100$ GeV are used to validate the background model and to normalize the Z+jets background. Figure 6 shows the reconstructed visible mass defined as the invariant mass of the sum of the two charged lepton four-momenta and the four-vector representing $\not{E}_T$. Figure 6 also shows the expected distribution for an RS graviton of mass $m_{G^*} = 325$ GeV overlaid.
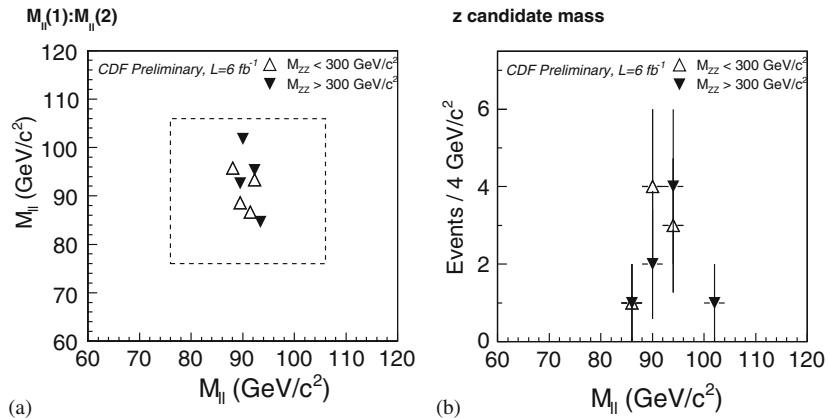

(a)

(b)

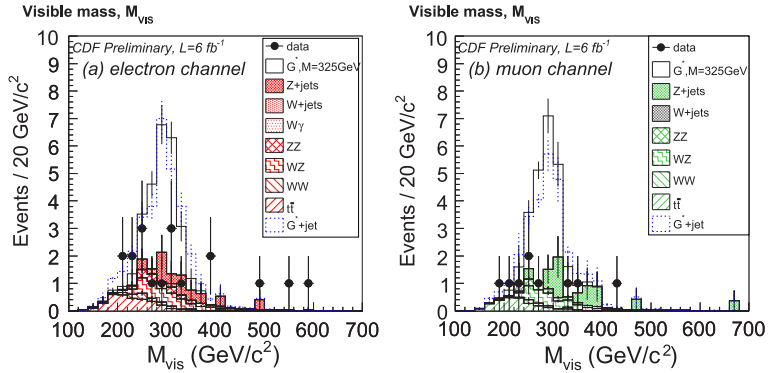**Figure 5.** Dilepton invariant mass distributions for the eight ZZ candidates.

Figure 6. Reconstructed visible mass for the $ll + \not{E}_T$ candidates. Overlaid is the signal for a graviton of mass $m_{G^*} = 325$ GeV (solid line) and a boosted graviton (dashed line).

Candidate events for the $ZZ \rightarrow l^+l^- jj$ process must have two leptons and two jets with $E_T > 20$ GeV. All pairs of jets are considered. If there is a pair with $70 < m_{jj} < 100$ GeV, it is accepted. The search for a high-mass resonance decaying to ZZ is optimized if the leading jet satisfies $E_T > 50$ GeV and p_T of either of the Z candidate is greater than 75 GeV. Figure 7 shows the reconstructed m_{lljj} distribution for the $eejj$ and the $\mu\mu jj$ channels, along with the prediction for a graviton (G^*) of mass $m_G = 325$ GeV with a production cross-section times branching fraction to ZZ of 1 pb that corresponds to the four-lepton excess. Motivated by the anomalous $p_T(ZZ)$ distribution shown by the events in the four-lepton channel, the signal selection is modified to require $p_T(jj) > 40$ GeV, which further suppresses Standard Model background. The data are found to be in good agreement with the expectations.

To quantify the results of the search, expected and observed limits on the production cross-section times branching ratio $\sigma(p\bar{p} \rightarrow X \rightarrow ZZ)$ are computed. Figure 8
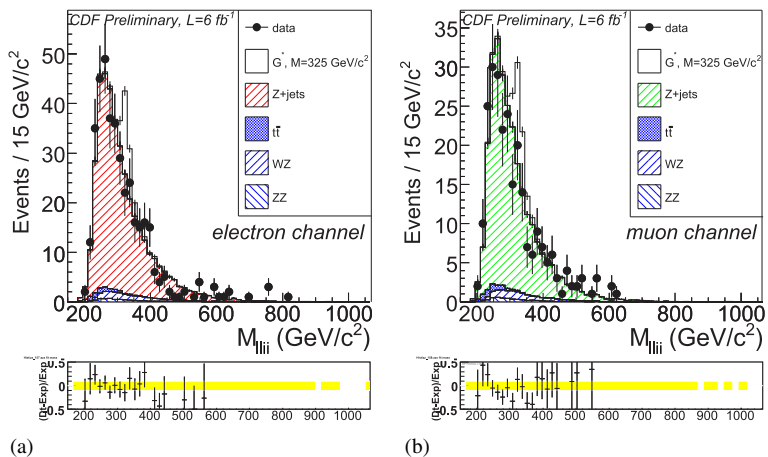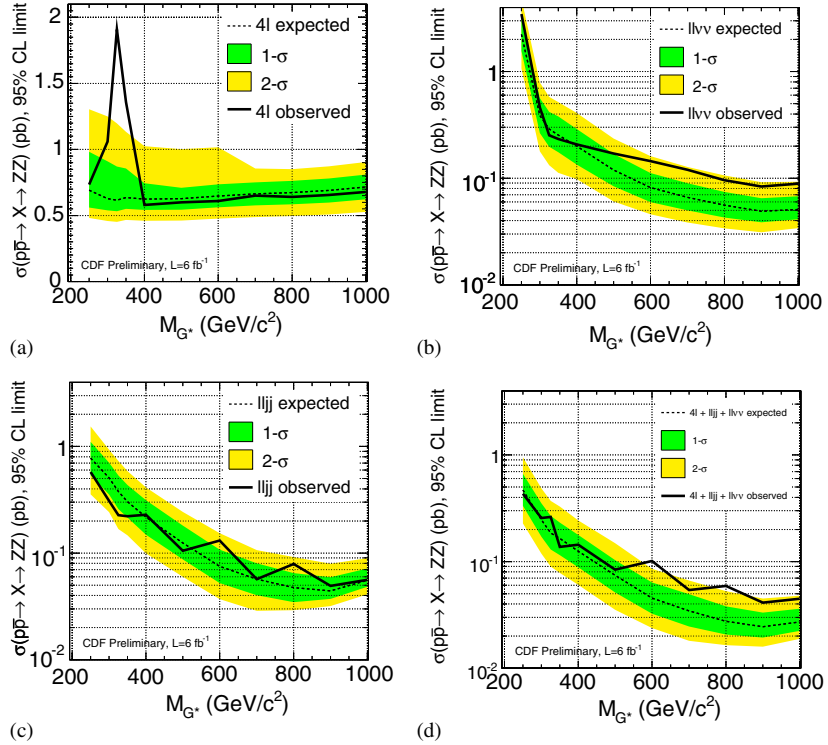

Figure 7. m_{lljj} distribution for (**a**) $eejj$ and (**b**) $\mu\mu jj$ channels

Figure 8. Expected and observed limits on the production cross-section times branching ratio $\sigma(p\bar{p} \to X \to ZZ)$. (**a**) Four-lepton channel; (**b**) leptons + $\not{E}_{\mathrm{T}}$ channel; (**c**) leptons + jets channel; (**d**) combined.

shows the expected and observed limits for G^* masses between 250 and 1000 GeV. Figure 8a shows the limits from the four-lepton channel. The four-candidate clusters around 327 GeV mass appear as a limit of 1.9 pb significantly higher than the expected limit. Figure 8b shows the limit from the leptons + $\not{E}_{\mathrm{T}}$ channel and figure 8c shows the limit from the leptons + jets channel. These two decay modes, despite the higher background, have a better sensitivity than the four-lepton channel. These modes do not present any excess of events and each of them excludes a resonance with a mass of 325 GeV with a cross-section larger than 0.26 pb. The combined limit is reported in figure 8d.

5.2 *D*0 *measurement of the ZZ production cross-section*

The D0 Collaboration measures the ZZ production cross-section in the cleanest four-lepton channel, using a data sample corresponding to an integrated luminosity of 6.4 fb^{-1} [21]. Events with four charged leptons (electrons or muons) are selected. Selection of events with four electrons or four muons requires E_{T} threshold of 30, 25, 15 and 15 GeV for each lepton. Instead, events with two electrons and two muons are selected if the leading electron and muon have $E_{\mathrm{T}} > 20$ GeV, and the sub-leading leptons have $E_{\mathrm{T}} > 15$ GeV. A total of 10 candidates are found. The distribution of the dilepton

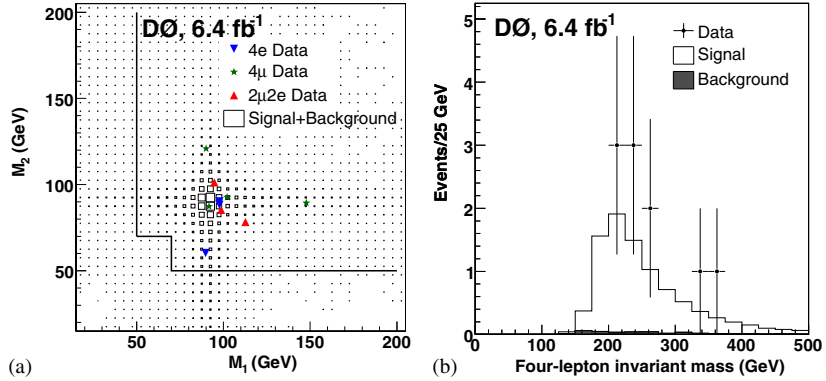**Figure 9.** (**a**) Invariant mass distribution for the two dilepton candidates. (**b**) Invariant mass distribution of the ZZ candidate.

invariant mass and of the four-lepton invariant mass are shown in figure 9. The data are found to be in good agreement with the expected ZZ background. The SM ZZ production cross-section is measured to be

$$\sigma(p\bar{p} \rightarrow ZZ) = 1.33^{+0.50}_{-0.40}\,(\text{stat.}) \pm 0.12\,(\text{syst.}) \pm 0.09\,(\text{lumi})\ \text{pb}.$$

The cross-section measurement is improved by combining it with the two leptons + $\not{E}_T$ channel and found to be

$$\sigma(p\bar{p} \rightarrow ZZ) = 1.40^{+0.43}_{-0.37}\,(\text{stat.}) \pm 0.14\,(\text{syst.})\ \text{pb}.$$

This is in good agreement with the SM NLO prediction of 1.4 ± 0.1 pb [22].

6. Search for fourth-generation neutrinos in $ZZ + \not{E}_T$ final state

In the final state with two Z bosons, the CDF Collaboration searched for the pair pro-
duction of fourth-generation neutrinos. The analysis is sensitive to a pair of unstable
fourth-generation neutrinos, each decaying into a Z and a stable ν. The event selection
requires fully reconstructed Z decays with two leptons and two jets in the final state, with
the additional requirement of large $\not{E}_T$. The $\not{E}_T$ threshold is optimized as a function of the
fourth-generation neutrino masses. No excess is found and upper limits of cross-section
are set as function of the two fourth-generation neutrino masses in the range 50 fb to
1 pb [23].

7. Search for anomalous triple gauge couplings

The electroweak symmetry breaking sector of the SM can be further tested to challenge
the SM and to search for deviation from it. In particular, triple gauge couplings (TGC)
can be anomalous if new physics effects include interactions between the gauge bosons.
The TGC have been analysed in all final states at the Tevatron. Recently, both D0 and

CDF realized new measurements of the WZ production cross-section and put limits on anomalous TGC in this channel that is sensitive to the WWZ coupling separately from the other couplings. Both analyses select events with three leptons (e or μ) and large $\not{E}_T$. The D0 Collaboration measures a production cross-section of $\sigma(WZ) = 3.90^{+1.01}_{-0.85}$ (stat.+ syst.) ± 0.31 (lumi) pb [24]. The CDF Collaboration measures a production cross-section of $\sigma(WZ) = 3.0^{+0.6}_{-0.5}$ (stat.)$^{+0.6}_{-0.4}$ (syst.) pb [25]. These results are in agreement with the SM NLO prediction of $\sigma(WZ) = 3.25 \pm 0.19$ pb [22]. The p_T of the Z candidate that is well measured is used to search for anomalous TGC that would enhance the cross-section at high p_T. No anomalous production is observed and limits are set on the anomalous TGC parameters [24,26].

8. Diboson with jets and Wjj anomaly

Measurements of associated production of a W boson and jets are fundamental probes of the electroweak sector of the Standard Model since several important processes share this signature, such as diboson production, associated production of a W and a light Higgs boson and searches for new phenomena. In the past years the Tevatron experiments have been able to observe the production of heavy bosons pairs with one vector boson decaying to a quark–antiquark pair. The D0 Collaboration has reported strong evidence of the production of $WW + WZ \rightarrow l\nu jj$ [27]. The CDF Collaboration observed the combined production of $WW + WZ + ZZ \rightarrow \not{E}_T + jj$ [28]. CDF has also observed production of $WW + WZ \rightarrow l\nu jj$ [29], both with and without multivariate techniques. This last analysis found a small excess of events, compatible with a statistical fluctuation, with a dijet invariant mass close to 150 GeV. The nature of this fluctuation was further investigated to determine whether it could be just a fluctuation, a hint of a small systematic effect, or the hint of a physical signal appearing as a dijet resonance [30]. The original analysis selection required a W candidate decaying leptonically into an electron or muon with $p_T > 20$ GeV and a neutrino reconstructed as $\not{E}_T > 25$ GeV. At least two jets with $E_T > 20$ GeV were required in addition to the W. The invariant mass of the two leading jets was used as a discriminating variable to search for the hadronically decaying W ($W \rightarrow jj$). Only events with transverse momentum of the dijet pair above 40 GeV have been retained, because these provide a better shape separation between the background and the $W \rightarrow jj$ signal. In order to adapt the analysis to search for a potential resonance of mass close to 150 GeV, the jet energy threshold was raised to 30 GeV to further reject the W+jets background and to reduce systematics associated with low-energy jets.

A combined binned χ^2 fit, for electron and muon events, to the dijet invariant mass m_{jj} spectrum is performed using predictions for the multijet QCD, WW, WZ, Z+jets, W+jets, $t\bar{t}$, and single top processes. The final W+jets normalization is determined by minimizing this χ^2 and all other contributions are constrained to be within the variance of their expected normalization. The fit to the dijet mass distribution in the range 28–300 GeV, in figure 10, shows that the model describes the data within uncertainties, except in the mass region $\approx$120–160 GeV, where an excess over the simulation is seen [30].

Since ref. [30], the result has been updated with more luminosity [31]. The excess is modelled with an additional Gaussian contribution and a $\Delta\chi^2$ test of hypothesis is performed. The width of the Gaussian is fixed to the expected dijet mass resolution by scaling
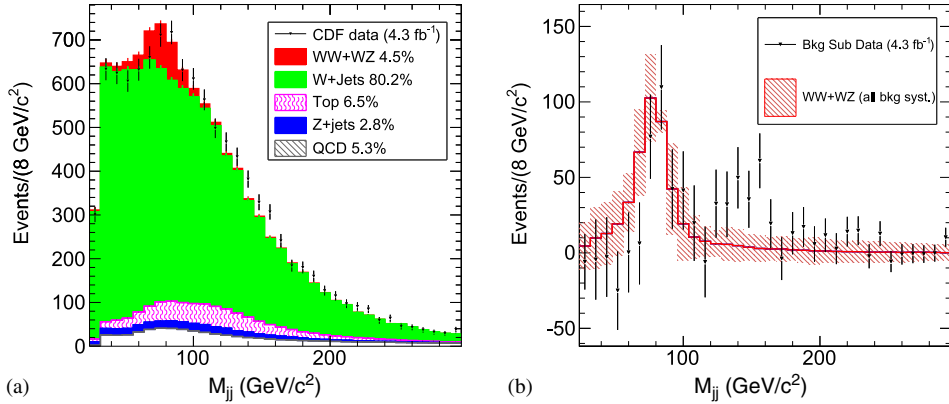
Figure 10. CDF dijet invariant mass distribution corresponding to an integrated luminosity of 4.3 fb^{-1}. The sum of electron and muon events is plotted. (**a**) shows the fit for known processes only and (**b**) shows, by subtraction, only the resonant contribution to M_{jj} including WW and WZ production.

the width of the W peak in the same spectrum: $\sigma_{\text{resolution}} = \sigma(W) \times \sqrt{(M_{jj}/M_{\text{W}})} = 14.3$ GeV, where σ_{W} and M_{W} are the resolution and the average dijet invariant mass for the hadronic W in the WW simulations respectively, and M_{jj} is the dijet mass where the Gaussian template is centred. In the combined fit, the normalization of the Gaussian is free to vary independently for the electron and muon samples, while the mean is constrained to be the same. The result of this fit is shown in figure 11. The fit finds an excess of 400 ± 70 events with a Gaussian mean of 147 ± 5 GeV (including only the statistical error). Assuming only background contributions, and systematic errors, the probability to
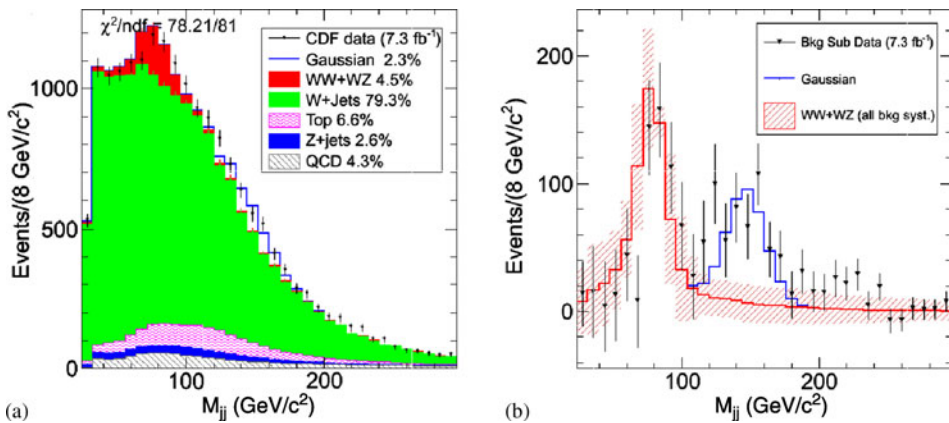

Figure 11. CDF dijet invariant mass distribution corresponding to an integrated luminosity of 7.3 fb^{-1}. The sum of electron and muon events is plotted. (**a**) shows the fit for known processes plus a hypothetical Gaussian component and (**b**) shows, by subtraction, only the diboson (WW, WZ) and hypothetical Gaussian contributions.

observe an excess larger than the one observed in the data is 1.9×10^{-5} corresponding to a significance of 4.1 standard deviations for a Gaussian distribution.

Multiple studies have been performed to understand the cause of the excess and are documented in ref. [31], in particular the same analysis has been performed without requiring strictly two jets, in order to exclude mismodelling due to the jet veto. Different NLO MC generators are used for top and single top, whose contribution are also doubled and still do not account for the excess. W+jets contribution is also simulated using SHERPA leading to a better description on the high mass tail and a smaller excess. While the main point of interest is to establish whether the excess is due to statistical, systematics effects or not, the observed excess matches well with the model proposed in [32].

8.1 *D*0 *analysis and comparison*

After the CDF article [30] was published, the D0 Collaboration analysed in detail the dijet mass distribution of W+jets events. The D0 analysis uses a selection that matches closely with the CDF one and observes good agreement between data and MC in a data sample of 4.3 fb^{-1} [33], while having sensitivity for the CDF excess. The result of the fit to the data and the background-subtracted data are shown in figure 12. Using $WH \rightarrow lvb\bar{b}$ with $M_{\rm H} = 150$ GeV as a model for the acceptance time efficiency, upper limits are determined for the cross-section time branching ratio of a hypothetical resonance produced in association with a W and decaying to dijets (see figure 13a). For a resonance mass $M_{jj} = 145$ GeV corresponding to the CDF excess, the p-value of the signal+background hypothesis as a function of hypothetical signal cross-section are shown in figure 13b. While some differences are present between the two analyses and the treatment of systematic uncertainties, one can proceed to make a direct comparison on the cross-section estimated using an acceptance and efficiency from a MC sample of WH with a Higgs mass of 150 GeV, and using the same luminosity. The cross-sections are 0.4 ± 0.8 pb and 3.1 ± 0.8 pb, respectively for D0 and CDF, leading to a difference between the two experiments of $\sim$2.5 standard deviations using Gaussian approximation for the errors.
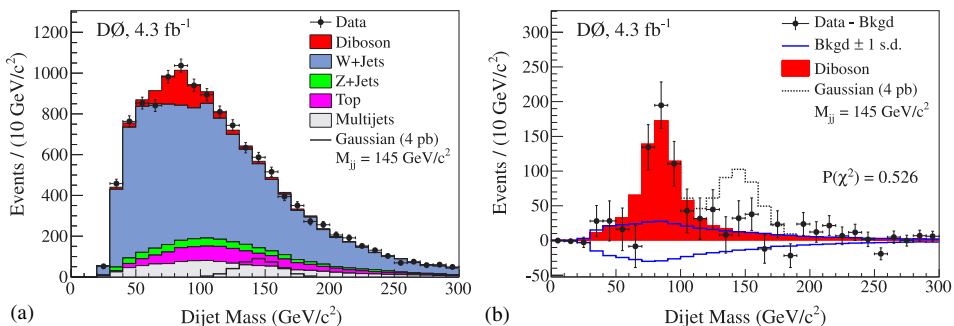

(a) (b)

Figure 12. Dijet invariant mass summed over electron and muon channels after the fit (**a**) without and (**b**) with subtraction of SM contributions other than that from the SM diboson processes. Also shown is the relative size and shape for a model with a Gaussian resonance with a production cross-section of 4 pb at $M_{jj} = 145$ GeV/c^2.
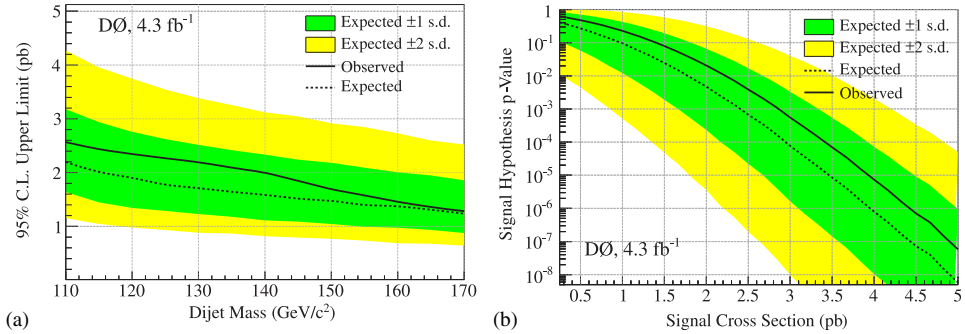
(a)

(b)

Figure 13. (**a**) Upper limits on the cross-section at the 95% CL for a Gaussian signal as function of dijet invariant mass. (**b**) Distribution of *p*-values for the signal+background hypothesis with a Gaussian signal with mean of $M_{jj} = 145$ GeV as a function of hypothetical signal cross-section.

In conclusion, the D0 analysis does not confirm the CDF excess. The results of the two experiments show a tension at the level of ~2.5 standard deviations.

9. Search for scalar top quark pair production

In the minimal supersymmetric Standard Model (MSSM) [34], the mixing between the chiral states of the scalar partners of the SM fermions is greatest for the partners of the top quark due to its large Yukawa coupling [35]. Thus, it is possible that the scalar top quark ($\tilde{t}_1$) is the lightest squark and has the largest production cross-section. If *R*-parity [36]
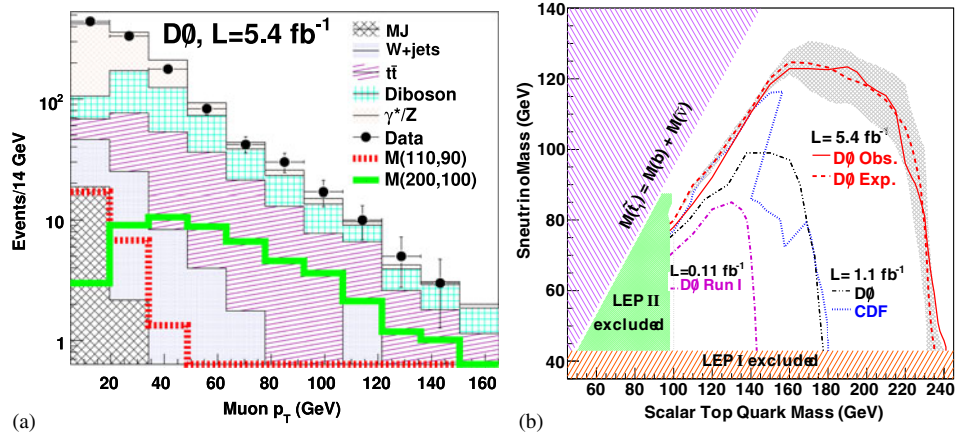

(a)

(b)

Figure 14. (**a**) Distribution of muon p_T comparing data and all background processes after initial selection. The thick dashed and thick solid lines represent signal benchmarks. (**b**) The observed (expected) 95% CL exclusion region includes all mass points below the solid (dashed) line.

is conserved, then scalar top quarks will be produced by $p\bar{p}$ collisions in pairs with the dominant processes being quark–antiquark annihilation and gluon fusion [35].

In ref. [37], the D0 Collaboration reports on a search for the production of $\tilde{t}_1\bar{\tilde{t}}_1$ pairs in the $b\bar{b}e^{\pm}\mu^{\mp}\tilde{\nu}\bar{\tilde{\nu}}$ final state using a data sample of 5.4 fb^{-1}. The analysis assumes that $\tilde{t}_1$ has a 100% branching fraction in this three-body decay mode with equal fraction to each lepton type, that R-parity is conserved, and that the sneutrino ($\tilde{\nu}$) is the lightest supersymmetric particle or decays invisibly into a neutrino and a neutralino ($\tilde{\chi}_1^0$). Events selected require: two jets with $E_{\mathrm{T}} > 20$ GeV, one electron with $E_{\mathrm{T}} > 15$ GeV, one μ with $E_{\mathrm{T}} > 10$ GeV and $\not{E}_{\mathrm{T}} > 7$ GeV. Figure 14a shows the good level of agreement between the data and the SM predictions. The selection is then refined using discriminant variables optimized to reject each of the main backgrounds ($Z/\gamma^* \rightarrow \tau\bar{\tau}$, WW, and $t\bar{t}$) as described in ref. [37]. Using a 2D signal-background discriminant, 95% confidence level (CL) limits in the plane $\tilde{\nu}$ mass vs. $\tilde{t}_1$ mass are determined. Stop pair production for $M_{\tilde{t}_1} < 210$ GeV is excluded when $M_{\tilde{\nu}} < 110$ GeV and the difference $M_{\tilde{t}_1} - M_{\tilde{\nu}} > 30$ GeV.

10. Search for new physics with same-sign dilepton final states

Final states with two leptons having the same charge are interesting because the SM background is very low, but they are a common signature for many beyond the SM models: SUSY, fourth generation, like-sign top quarks or doubly charged bosons. The CDF Collaboration searched for these signals in a data sample of 6.1 fb^{-1} starting from a common selection that requires a trigger lepton (e or μ) with $p_{\mathrm{T}} > 20$ GeV, a second lepton (e or μ) with $p_{\mathrm{T}} > 10$ GeV, dilepton invariant mass $M_{ll} > 25$ GeV and vetoing events from the Z decay. The data are found to be consistent with the SM [38]. At 95% CL, upper limits on like-sign top quark production $\sigma(uu \rightarrow tt) \times \mathrm{BR}(W \rightarrow l\nu)^2 \lesssim 50$ fb are set depending on the chirality mode [39]. Upper limits on the production of squarks and gluinos (or UED equivalent) are determined as a function of the new particle masses [40].

The dilepton invariant mass distribution is found to be consistent with the SM. Lower limits at 95% CL are set on the mass of doubly-charged scalars decaying to like-sign dileptons, $m_{\mathrm{H}^{\pm\pm}} > 190$–245 GeV, depending on the decay mode and coupling [41]. The search is also performed in the final state with one τ lepton in order to increase the sensitivity at high $\tan(\beta)$. Again the data are found to be in good agreement with the SM. At 95% CL, $M_{\tilde{\chi}^{\pm}} \lesssim 130$–310 GeV is excluded depending on the model, as described in ref. [42].

11. Search for charged massive long-lived particles

The D0 Collaboration searches for charged massive long-lived particles (CMLLP) in a data sample of 5.2 fb^{-1}. This search is model-independent and looks for a particle that traverses the detector (like a muon), but has slower speed (low β) and larger ionization energy loss. The search uses a boosted decision tree discriminant. The data are found to be in good agreement with the SM. Stops with $M_{\tilde{t}} < 265$ GeV, wino-like charginos with $M_{\tilde{\chi}^{\pm}} < 251$ GeV and higgsino-like charginos with $M_{\tilde{\chi}^{\pm}} < 230$ GeV are excluded. These are the current best limits for a stable chargino [43].

12. Conclusions

The Tevatron has looked for new physics in a wide range of final states with data samples up to 9 fb^{-1} analysed so far. There are a few hints that are being followed up on, while the full dataset is being analysed. All CDF and D0 results are available in refs [44,45].

References

[1] CDF-II Collaboration: R Blair *et al*, The CDF-II detector: Technical design report (1996), FERMILAB-DESIGN-1996-01, FERMILAB-PUB-96-390-E
[2] CDF Collaboration: D Acosta *et al*, *Phys. Rev.* **D71**, 032001 (2005), hep-ex/0412071
[3] D0 Collaboration: V M Abazov *et al*, *Nucl. Instrum. Methods* **A565**, 463 (2006), physics/0507191
[4] D0 Collaboration: R Angstadt *et al*, *Nucl. Instrum. Methods* **A622**, 298 (2010), arXiv:0911.2522
[5] T Sjostrand, P Eden, C Friberg, L Lonnblad, G Miu *et al*, *Comput. Phys. Commun.* **135**, 238 (2001), hep-ph/0010017
[6] M L Mangano, M Moretti, F Piccinini, R Pittau and A D Polosa, *J. High Energy Phys.* **0307**, 001 (2003), hep-ph/0206293
[7] E Boos *et al*, *PoS* **ACAT08**, 008 (2008), arXiv:0901.4757
[8] H L Lai *et al*, *Eur. Phys. J.* **C12**, 375 (2000), hep-ph/9903282
[9] J Pumplin *et al*, *J. High Energy Phys.* **07**, 012 (2002), hep-ph/0201195
[10] S Weinberg, *Eur. Phys. J.* **C34**, 5 (2004), hep-ph/0401010
[11] Particle Data Group: K Nakamura *et al*, *J. Phys.* **G37**, 075021 (2010)
[12] D0 Collaboration: V M Abazov *et al*, *Phys. Rev.* **D84**, 071104 (2011), arXiv:1107.1849
[13] L Randall and R Sundrum, *Phys. Rev. Lett.* **83**, 3370 (1999), hep-ph/9905221
[14] D0 Collaboration: V M Abazov *et al*, *Phys. Rev. Lett.* **104**, 241802 (2010), arXiv:1004.1826
[15] CDF Collaboration: T Aaltonen *et al*, *Phys. Rev. Lett.* **107**, 051801 (2011), arXiv:1103.4650
[16] http://www-cdf.fnal.gov/physics/exotic/r2a/20110603.fullgraviton/index.html (2011)
[17] D0 Collaboration: V M Abazov *et al*, *Phys. Rev. Lett.* **107**, 011801 (2011), arXiv:1011.6278
[18] G Altarelli, B Mele and M Ruiz-Altaba, *Z. Phys.* **C45**, 109 (1989)
[19] CDF Collaboration: T Aaltonen *et al*, *Phys. Rev.* **D85**, 012008 (2012), arXiv:1111.3432
[20] M Kober, B Koch and M Bleicher, *Phys. Rev.* **D76**, 125001 (2007), arXiv:0708.2368
[21] D0 Collaboration: V M Abazov *et al*, *Phys. Rev.* **D84**, 011103 (2011), arXiv:1104.3078
[22] J M Campbell and R K Ellis, *Phys. Rev.* **D60**, 113006, (1999), hep-ph/9905386
[23] http://www-cdf.fnal.gov/physics/exotic/r2a/20110603.zzmet/index.html (2011)
[24] D0 Collaboration: V M Abazov *et al*, *Phys. Lett.* **B695**, 67 (2011), arXiv:1006.0761
[25] http://www-cdf.fnal.gov/physics/ewk/2011/wz/PublicPages/WZwebpage.html (2011)
[26] http://www-cdf.fnal.gov/physics/ewk/2011/WZatgc71/ (2011)
[27] D0 Collaboration: V M Abazov *et al*, *Phys. Rev. Lett.* **102**, 161801 (2009), arXiv:0810.3873
[28] CDF Collaboration: T Aaltonen *et al*, *Phys. Rev. Lett.* **103**, 091803 (2009), arXiv:0905.4714
[29] CDF Collaboration: T Aaltonen *et al*, *Phys. Rev. Lett.* **104**, 101801 (2010), arXiv:0911.4449
[30] CDF Collaboration: T Aaltonen *et al*, *Phys. Rev. Lett.* **106**, 171801 (2011), arXiv:1104.0699
[31] http://www-cdf.fnal.gov/physics/ewk/2011/wjj/7_3.html (2011)
[32] E J Eichten, K Lane and A Martin, *Phys. Rev. Lett.* **106**, 251803 (2011), arXiv:1104.0976
[33] D0 Collaboration: V M Abazov *et al*, *Phys. Rev. Lett.* **107**, 011804 (2011), arXiv:1106.1921
[34] S Dimopoulos and H Georgi, *Nucl. Phys.* **B193**, 150 (1981)
[35] W Beenakker, M Kramer, T Plehn, M Spira and P M Zerwas, *Nucl. Phys.* **B515**, 3 (1998), hep-ph/9710451

[36] P Fayet and S Ferrara, *Phys. Rep.* **32**, 249 (1977)
[37] D0 Collaboration: V M Abazov *et al*, *Phys. Lett.* **B696**, 321 (2011), Long author list - awaiting processing, arXiv:1009.5950
[38] http://www-cdf.fnal.gov/physics/exotic/r2a/20110407.samesigndileptons/index.html (2011)
[39] http://www-cdf.fnal.gov/physics/exotic/r2a/20110407.samesigndileptons/sstops.html (2011)
[40] http://www-cdf.fnal.gov/physics/exotic/r2a/20110407.samesigndileptons/susy.html (2011)
[41] CDF Collaboration: T Aaltonen *et al*, *Phys. Rev. Lett.* **107**, 181801 (2011), arXiv:1108.0101
[42] http://www-cdf.fnal.gov/physics/exotic/r2a/20110809_sstau/Home.html (2011)
[43] D0 Collaboration: V M Abazov *et al*, *Phys. Rev. Lett.* (2011), arXiv:1110.3302
[44] http://www-d0.fnal.gov/Run2Physics/WWW/results.htm
[45] http://www-cdf.fnal.gov/physics/physics.html